

Design and Comparison of Vector and Direct Torque Control of 3-Phase Induction Motor Drive

B. Vamsi Krishna

Department of Electrical and Electronics Engineering,
Bharath University, Chennai, India

Abstract: The aim of this paper is to design and compare the performance of vector and direct torque control of 3-phase Induction motor drive using Matlab/Simulink tool and In conventional vector and direct torque control (DTC) has, over the years, become of the most popular methods of control for induction motors (IM) drive system. In DTC a single stator voltage vector of the inverter standard topology is selected every control sampling period and it is maintained for the whole period. This makes the torque and stator flux reference values to be reached quickly, with a small number of inverter switching, resulting in a very good dynamic response. However, by this switching technique, based on hysteresis, large and small torque and flux errors are not distinguished, which cause an extra torque ripple in motor steady state operation According to the simulation, it can be verified that this Method not only Decrease the oscillation of torque and flux, but can simplify the design of control system as well. The analysis has been based both on an analytical and experimental approach. The results have shown that the vector control method, compared to the direct torque control of three phase induction motor drive. The direct comparison of the performances of the motor control technique has been made both for constant load and constant dissipated power conditions.

Key words: Induction Motor • Vector control • Direct torque control • Torque Ripple • Hysteresis controller • Switching Frequency

INTRODUCTION

The induction motor drives with squirrel cage-type have been the workhorses in industry for variable speed applications in a wide power range that covers from fractional horse power to the multi mega-watts because of their ruggedness and low cost [1]. The control and estimation of ac drives in general more complex than those of dc drives and this complexity increase substantially if high performance is needed. The main reason for this complexity in the control of induction motor are the need of variable frequency, harmonically optimum converter power supplies and the difficulties of processing feedback signals in the presence of harmonics [2]. The induction motor (IM) thanks to its well known advantages of simple construction, reliability, ruggedness and low cost has found very wide industrial applications. These advantages are superseded by control problems when using an IM in industrial drives with high Performance demands [3].

Ideally, a vector control of an induction motor drive operates like a separately excited dc motor drive. In a dc machine, neglecting the armature reaction and field saturation, the developed torque is given by:

$$T_e = K_t I_a I_f \quad (1)$$

where I_a = armature current, I_f = field current. The construction of a dc machine is such that the field flux ψ_f produced by the current I_f is perpendicular to the armature flux ψ_a produced by the armature current I_a . These space vectors, which are stationary in space, are orthogonal or decoupled in nature [4]. This means that when torque is controlled by controlling the current I_a , the flux ψ_f is not affected and we get fast transient response and high torque/ampere ratio with rated ψ_f . When the field current I_f is controlled, it affects the field flux only, but not armature flux. Because of inherent coupling problem an induction motor cannot generally give such a fast response [5].

Dc machine like performance can also be extended to an induction motor if the machine controls is considered in a synchronously rotating reference frame (d^e-q^e), where the sinusoidal variable appear as dc quantities in a steady state. The control current inputs, i_{ds}^* and i_{qs}^* . These are the direct axis component and quadrature axis component, respectively, in asynchronously rotating reference frame. with vector control, i_{ds} is analogous to the field current and i_{qs} is analogous to armature current i_a of a dc machine. Therefore the torque can be expressed as:

$$T_e = K_t i_{ds} i_{qs} \quad (2)$$

This means that when i_{qs}^* controlled, it affects the actual i_{qs} current only, but does not affect the flux Ψ_r . Similarly when i_{ds}^* is controlled it controls the flux only and does not affect the i_{qs} component of current [6]. Based on the method of generation of the unit vector for finding the speed of rotation of the synchronous frame, the vector control is classified as direct or indirect method. The speed of rotation is directly found from the machine model or the estimator in the case of direct vector control, whereas in the case of indirect vector control it is found by adding the rotor speed with help of slip speed. The reduced version of the Vector control is Direct Torque Control [7].

Direct Torque Control (DTC) is emerging technique for variable speed control of inverter driven induction motor. This method allows the direct control of stator flux and instantaneous torque through simple algorithm. Basically, it uses torque and stator flux control loops, where the feedback signals are estimated from the machine terminal voltages and currents. The torque command can be generated by the speed loop. The loop errors are processed through hysteresis bands and fed to a voltage vector look-up table. The flux Control loop has outputs +1 and -1, whereas the torque Control loop has three outputs, +1, 0 and -1. The inverter voltage vector table also gets the information about the location of the stator flux vector. From the three inputs, the voltage vector table selects an appropriate voltage vector to control the PWM inverter switches. This is analogous to the hysteresis based current control in the case of vector control. Due to the absence of several controllers and the transformations in DTC, the delay in processing signal is drastically reduced [8].

Because of the simplicity and superior performance of DTC make it more popular in industrial applications, if some of the disadvantages like high ripple, variable

switching frequency are removed. The principle of operation of vector control and DTC control is detail in the next Topics.

Vector Control: The vector control based on current controlled PWM inverter which is very popular method used in industry. The fundamentals of vector control implementation can be explained with the help of Figure 1, where the machine model is represented in a synchronously rotating reference frame. Assume that the inverter has unity current gain, that is, it generates currents i_a, i_b, i_c as dictated by the corresponding command current i_a^*, i_b^*, i_c^* from the controller. A machine model with internal conversions is shown on the right. The machine terminal phase currents i_a, i_b, i_c are converted to i_{ds}^s, i_{qs}^s components by $3\Phi/2\Phi$ transformation. These are then converted to synchronously rotating frame by the unit vector components $\cos \theta_e$ and $\sin \theta_e$ before applying them to the d^e-q^e model as shown. The transformation equations will be given later in this chapter. The controller makes of inverse transformation as shown so, that the control currents i_{ds}^* and i_{qs}^* correspond to the machine currents i_{ds} and i_{qs} respectively. In addition the unit vector assures correct alignment of i_{ds} , current with the flux vector Ψ_r . There are essentially two general methods of vector control. One is direct control and other is indirect control depends on the how unit vector is generated for the control [9].

The key component of the Field oriented control (FOC) strategy is the Clarke and Park transform blocks. These map the three phase stator currents onto a direct and quadrature rotating reference frame that is aligned with the rotor flux. This decouples the torque and flux producing components of the stator currents allowing the induction motor to be controlled in much the same was as a separately excited DC machine. The d-axis component of the stator current is related to the rotor flux magnitude via Equation below.

$$\Psi_{dr} = L_m * i_{ds} \quad (3)$$

where, L_m is mutual inductance of the motor.

In the indirect vector control the unit vectors are in feed forward manner. The fundamental principle of indirect vector control is explained with the help of phasor diagram as shown in Figure 2. With the help of phasor diagram. The d^e-q^e axes are fixed on the stationary but the d^r-q^r axes, which are fixed on the rotor are moving at speed ω_r as shown. Synchronously rotating axes d^e-q^e

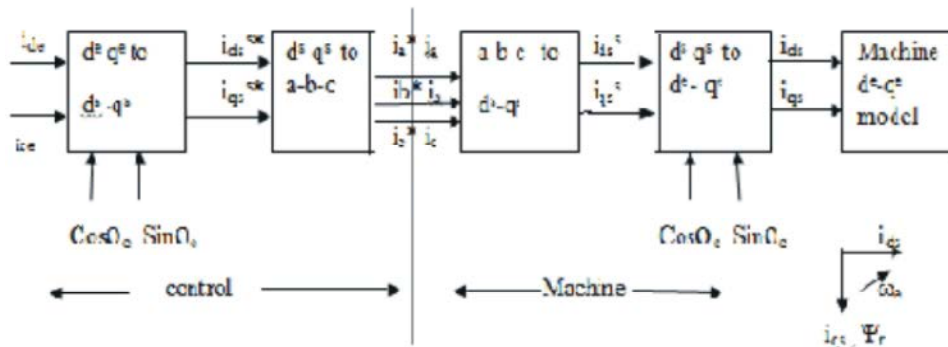


Fig. 1: Vector control implementation principle with machine d^o – q^o model

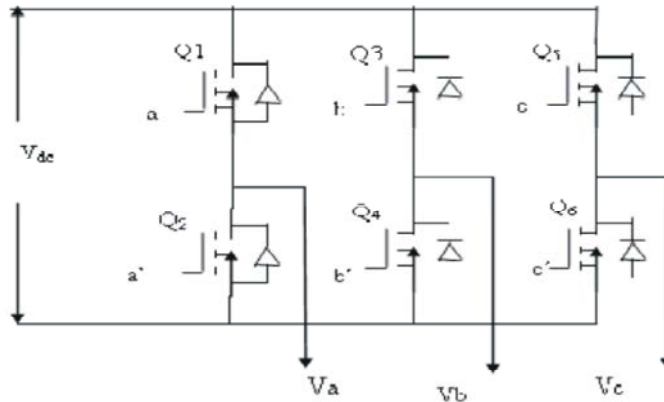


Fig. 2: Basic Three Phase Voltage Source Inverter

are rotating ahead of the d^r – q^r axes by the positive slip angle θ_{sl} corresponding to slip frequency ω_{sl} . Since the rotor pole is directed on the d^e axis and $\omega = \omega_r + \omega_{sl}$, we can write

$$\theta_e = \int \omega_e dt = \int (\omega_r + \omega_{sl}) dt = \theta_r + \theta^{sl} \quad (4)$$

The rotor pole position is not absolute, but is slipping with respect to the rotor at frequency ω_{sl} . The phasor diagram suggests that for decoupling control, the stator flux component current i_{ds} should be aligned on the d^e axis and the torque component of current i_{qs} should be on the q^e axis.

For decoupling control it is desirable that $\Psi_{qr} = 0$, That is,

$$d\Psi_{dr}/dt = 0 \quad (5)$$

So that the total rotor fluxes Ψ_r is directed on the d^e axis.

Then,

$$(L_r / \Psi_r) * (d\Psi_r / dt) + \Psi_r = L_m * i_{ds} \quad (6)$$

$$\omega_{sl} = ((L_m * R_r) / (L_r * \Psi_r)) * i_{qs} \quad (7)$$

where, $\Psi_r = \Psi_{dr}$ has been substituted.

If rotor flux $\Psi_r = \text{constant}$, which is usually the case then from equation (6).

$$\Psi_r = L_m * i_{ds} \quad (8)$$

In other words the rotor flux is directly proportional to current i_{ds} .

Overview of Space Vectors: Representing three phase quantities as Space Vectors is particularly useful for power electronic applications. Essentially this methods defines a three phase system with a single unity vector:

$$u_s = (1 + a + a^2) \quad (9)$$

where $a = e^{j2\pi/3}$

Using this unity vector, a space vector representation of phase voltages v_a, v_b, v_c is therefore:

$$V = (2/3) (v_a + a v_b + a^2 v_c) \quad (10)$$

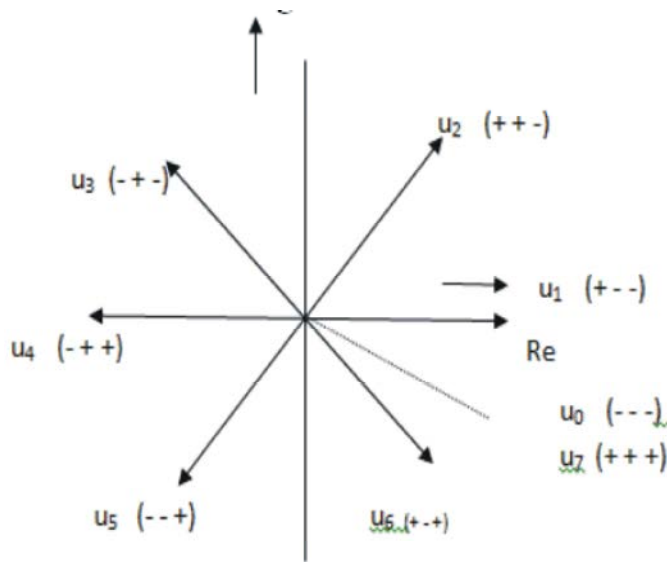


Fig. 3: Switching Voltage Space Vectors

Table 2.1: Space vector switching pattern

a	b	c	Va	Vb	Vc	Vab	Vbc	Vca
0	0	0	0	0	0	0	0	0
1	0	0	2/3	-1/3	-1/3	1	0	-1
1	1	0	1/3	1/3	-2/3	0	1	-1
0	1	0	-1/3	2/3	-1/3	-1	1	0
0	1	1	-2/3	1/3	1/3	-1	0	1
0	0	1	-1/3	-1/3	2/3	0	-1	1
1	0	1	1/3	-2/3	1/3	1	-1	0
1	1	1	0	0	0	0	0	0

The 2/3 scaling factor is necessary to ensure that the system remains power invariant.

The Space Vector Switching Pattern: There are eight possible combinations of switching patterns for the three upper MOSFETs of the inverter switching legs. The phase and line to line voltages generated by each of these combinations can be calculated from equation and are expressed as a fraction of V_{dc} . The results of this are presented in Table 2.1.

For each switching combination a voltage space vector can be constructed using the phase voltages and equation (10) When these space vectors are plotted on a set of real and imaginary axes the switching diagram in Figure (3) is obtained. The switching space vectors divide the axes into 6 equally sized sectors. The two null vectors 000 and 111 are located at the origin.

Generating a Reference Voltage: The objective of SVPWM is to approximate a reference space vector V_{ref} , somewhere within the transcribed circle of Figure (4) using a combination of the eight switching vectors. One method is to set the average voltage of the inverter

over a time period T_{pwm} to be equal to the average voltage of the reference space vector in that period. This is done by time modulating the two adjacent switching vectors that set the bounds for the sector the reference vector is currently in. The binary representation for two adjacent switching vectors differs by one bit so only one of the upper transistors needs to change. This improves the inverter's performance and significantly simplifies the digital implementation of the algorithm.

If we assume that the switching frequency is high and that the change in V_{ref} over this period is small then the modulation scheme can be represented using the following equation:

$$T_{pwm} V_{ref} = 2/3(T1V_{switch x} + T2 V_{switch x+1} + T3 V_{Null}) \quad (11)$$

where $V_{switch x}$ and $V_{switch x + 1}$ represent the adjacent switching vectors for sector x. V_{Null} is the null switching vector and T1, T2 and T3 are the durations for each switching vector. The sum of T1 and T2 is less than or equal to V_{ref} so the null vector V_{Null} is activated for time T3 to make up the rest of the switching period such that:

$$T_{pwm} = T1 + T2 + T3 \quad (12)$$

The length of the reference vector determines the magnitude of the output voltage, while the speed with which the vector rotates around the circle determines the frequency of the three phase system. In a motor application the direction of the rotor depends on whether the reference vector is rotating clockwise or anti-clockwise.

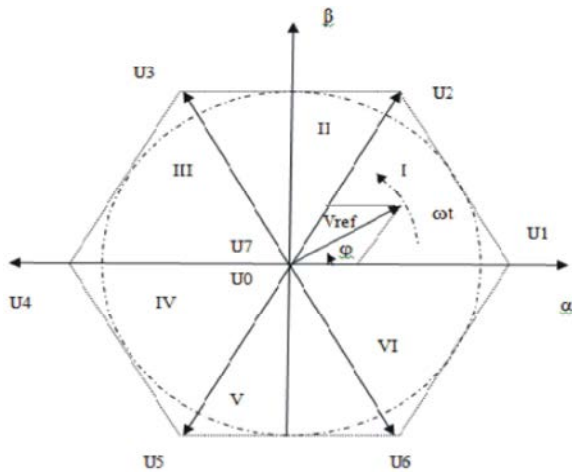


Fig. 4: V_{ref} Mapped onto the Switching Pattern

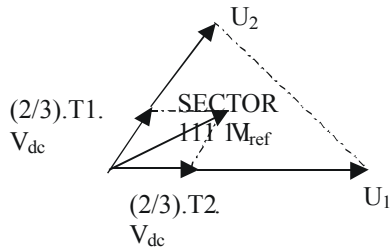


Fig. 5: Generating V_{ref} in Sector 1

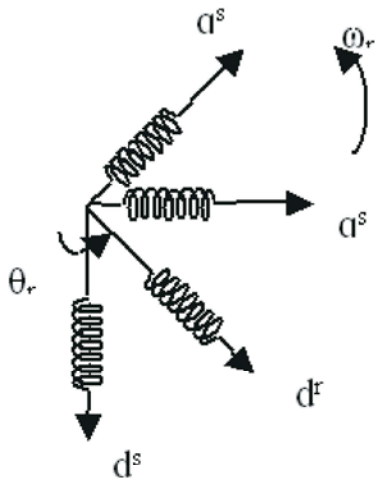


Fig. 6: Equivalent two-phase machine for 3-phase machine

Dynamic D-Q Model of Induction Machine: Vector control is based on the dynamic d-q model of the machine. The dynamic performance of an ac machine is somewhat complex because the three-phase rotor windings move continuously with respect to three-phase stator windings. The machine model can be described by differential equations with time varying mutual inductance, but such a model tends to be very complex. The three phase machine can be represented by an equivalent two-phase

machine as shown in Figure (6). Where d^s - q^s corresponds to stator direct and quadrature axes and d^r - q^r corresponds to the rotor direct and quadrature axes.

In this two-phase model the time varying inductances can be eliminated by referring the stator and rotor variables to a common reference which may rotate at any speed.

Synchronously rotating d^c - q^c axes rotates at synchronous speed ω_e with respect to the d^s - q^s axes and the angle $\theta_e = \omega_e t$. The two phase d^s - q^s windings are transformed into the hypothetical windings mounted on the d^c - q^c axes. The voltage on the d^c - q^c axes can be converted into the d^c - q^c axes as follows:

$$V_{qs}^c = v_{qs}^s \cos \theta_e - v_{ds}^s \sin \theta_e \quad (13)$$

$$V_{ds}^c = v_{qs}^s \sin \theta_e + v_{ds}^s \cos \theta_e \quad (14)$$

Again resolving the synchronously rotating frame parameters into a stationary frame the relation are:

$$V_{qs}^s = v_{qs}^c \cos \theta_e + v_{ds}^c \sin \theta_e \quad (15)$$

$$V_{ds}^s = -v_{qs}^c \sin \theta_e + v_{ds}^c \cos \theta_e \quad (16)$$

Direct Torque Control: Direct Torque Control (DTC) is an entirely different approach to induction motor control that was developed to overcome Vector Control's relatively poor transient response and reliance on induction motor parameters. The standard closed loop Vector Control structure consists of

- A number of coordinate transforms to decouple flux and torque
- A current model to estimate the rotor flux angle
- Two PI controllers for the direct and quadrature currents
- An additional PI controller to regulate the speed.

In DTC the first three components are removed and replaced by two hysteresis comparators and a look up table. Another benefit is that it can calculate torque without the need for complex observer algorithms or mechanical speed sensors.

Principle of Operation of Direct Torque Control: In the Direct Torque Control method instead of using coordinate transforms and PI controllers to determine the output reference voltages for the inverter, it uses a look up table. Flux and torque are used as feedback signals for the controller. The errors in torque, stator flux magnitude and

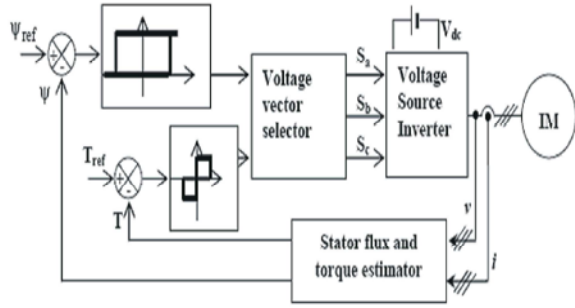


Fig. 7: Block diagram of Direct torque & Flux control method

angle are used as the inputs for this table. Each of these variables is discretised into a specific number of levels using a hysteresis comparator. The error in magnitude of the stator flux is 1 if it is low and 0 otherwise. Torque error is represented using three levels with -1 being too high, 0 being acceptable and 1 being too low. Finally the stator flux angle is discretised into six, 60 degree sectors corresponding to the regions bounded by the PWM space vectors. The block diagram of the Direct Torque control Induction Motor drive is shown in Figure (7).

$$\psi_s = \int (v_s - R_s i_s) dt \quad (17)$$

The d and q components of ψ_s are given by:

$$\psi_{ds} = \int (v_{ds} - R_s i_{ds}) dt \quad (18)$$

$$\psi_{qs} = \int (v_{qs} - R_s i_{qs}) dt \quad (19)$$

The electromagnetic torque is an important output variable that determines such mechanical dynamics of the machine as the rotor position and speed. The electromagnetic torque of an induction motor in stator reference frame is given by:

$$T_e = \frac{3}{2} \frac{p}{2} [i_{qs} \lambda_{ds} - i_{ds} \lambda_{qs}] \quad (20)$$

We can estimate the electromagnetic torque of induction motor:

Flux and Torque Hysteresis Controllers: The diagram for direct torque and flux control is shown in Figure (6) The command stator flux Ψ_{s^*} and torque t_e^* magnitudes are compared with the respective estimated values and the errors are processed through hysteresis band controllers. As shown. The flux loop controller has two levels of digital output according to the following equations.

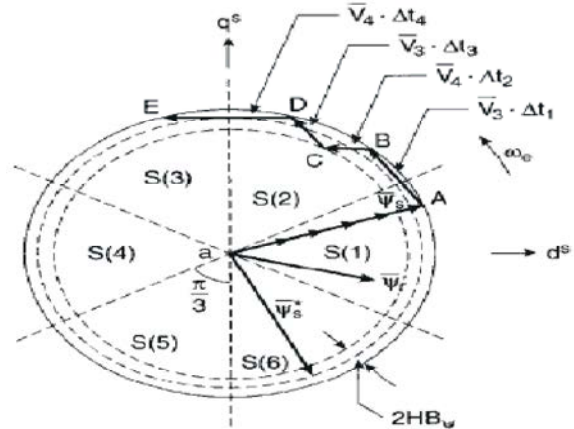


Fig. 8: Trajectory of stator flux vector in DTC control

$$H_{\psi} = 1 \text{ for } E_{\psi} > +HB_{\psi} \quad (21)$$

$$H_{\psi} = -1 \text{ for } E_{\psi} < -HB_{\psi} \quad (22)$$

where,

$2HB_{\psi}$ = total hysteresis band width of the flux controller.

The circular trajectory of the command flux vector Ψ_{s^*} with hysteresis band rotates in anti-clock wise direction, as shown in Figure (8).

The actual stator flux Ψ_s within the hysteresis band and it tracks the command is constrained flux in zigzag path. The torque control loop has three levels of digital output as follows:

$$H_{T_e} = 1 \text{ for } E_T > +HB_T \quad (23)$$

$$H_{T_e} = -1 \text{ for } E_T < -HB_T \quad (24)$$

$$H_{T_e} = 0 \text{ for } -HB_T < E_T < +HB_T \quad (25)$$

The feedback flux and torque are calculated from the machine terminal voltage and currents.

Optimal Switching Logic: The sector number S (K) is also calculated from signal commutation block in which the flux vector Ψ_s lies. There are six sectors, each 60 degree angle wide, as shown in Figure (8) The voltage vector table block receives the input signals H_{ψ} , H_{T_e} and S(K) and generates the appropriate voltage vector for the inverter by a look up table which is shown in Table (2) Neglecting the stator resistance R_s of the machine, we can write:

$$\Delta \Psi_s = V_s * \Delta t \quad (26)$$

Table 2: Switching table of inverter voltage

H_{Ψ}	H_{T_e}	S(1)	S(2)	S(3)	S(4)	S(5)	S(6)
1	1	V2	V3	V4	V5	V6	V1
1	0	V0	V7	V0	V7	V0	V7
1	-1	V6	V1	V2	V3	V4	V5
-1	1	V3	V4	V5	V6	V1	V2
-1	0	V7	V0	V7	V0	V7	V0
-1	1	V5	V6	V1	V2	V3	V4

Which means that Ψ_s can be changed incrementally by applying stator voltage vector V_s , for time increment Δt .

The voltage vector look-up table for DTC control is shown in table for the three inputs H_{Ψ} , H_{T_e} and S (K). Depending upon these three input signals the inverter gets respective voltage vector. The zero vector short circuits the machine terminal and keeps the flux and torque essentially unchanged.

RESULTS AND DISCUSSIONS

The Complete model of Vector and Direct Torque Control of induction motor drive is developed by Matlab/Simulink tool box. The major problems associated with Vector Control drive is feedback signal estimation is complex and it requires a number of coordinate transformations. The DTC induction motor drive provides superior performance and here is no need of coordinate transformation. The main drawback of DTC drive is the flux and torque ripples. This chapter briefly discusses the simulation results of the Vector and Direct Torque Control induction motor drive.

Motor Parameters: The rating and parameters of the induction machine and inverter data used for simulation are given in Table (3) and (4).

The Matlab/Simulink implementation of conventional Vector Control induction motor drive is shown in Figure 9. The three phase quantities are converted into two phase quantities and vice versa by using Clark and Park transformations. The simulated waveforms of stator current, electromagnetic torque and rotor speed (rad/sec) was shown in Figure 10.

The reference speed given is 100 rad/sec. After 0.75 seconds the step given to the reference speed is 150 rad/sec. The corresponding changes in rotor speed, stator current and electromagnetic torque was shown in Figure 10. After reaching rotor speed to its reference speed the electromagnetic torque settles to the rated value.

Table 3: Parameters of 3HP 460V, 50Hz 4 Pole Induction Machine

Parameter	Values
Stator Resistance (R_s)	1.115 Ω
Rotor Resistance (R_r)	1.083 Ω
Stator Inductance (L_s)	0.005974mH
Rotor Inductance (L_r)	0.005974mH
Magnetizing Inductance (L_m)	0.0347mH
Inertia (J)	0.02Kg/m ²
Rated Current	5.0 Amp
Rated Torque	22.38 Nm
Rotor speed	1500 rpm

Table 4: Inverter Data

Electrical Quantity	Rating
Power	3 KW
Voltage	460V -AC

Table 5:

Parameter	Vector Control	DTC
Torque Ripple (N-m)	-0.2 to 1.08	-1.7 to 1.7
Flux ripple (Wb)	0.19 to 0.4	0.97 to 1.2

The ripples in the electromagnetic torque at the steady state i.e. rotor speed settles to its reference speed were shown in Figure (11). In the steady state electromagnetic torque should be the one. Figure (12) shows the stator flux ripples and Figure (13) shows the stator q-axes and d-axes fluxes which can be controlled independently.

The simulated waveform of stator flux in d-q plane is shown in Figure 15. The stator d-axes flux was measured on the x-axes and stator q-axes flux was measured on y-axes and the corresponding graph was shown in Figure 15. The circular trajectory of flux vector rotates in anti-clock wise direction with the hysteresis band.

Simulated waveforms of stator current, electromagnetic torque and rotor speed shown in Figure (16) The reference speed was 100 rad/sec. The actual speed of the rotor settled to its reference speed in 0.26 seconds. After reaching the rotor speed to its reference speed the electromagnetic torque becomes zero. In the steady state the ripples in the electromagnetic torque and stator flux was shown in Figure (17) and (18) respectively. The torque ripples is between -1.7 to 1.7 and the stator flux ripples is between 0.97 to 1.2. And these values are tabulated in Table (5) and compared with vector control induction motor drive [10-13].

Comparison of Results: The Matlab/Simulink simulated results of the Torque ripples and stator flux ripples in steady state for the Vector and Direct Torque control of induction motor drive is tabulated in Table (5).

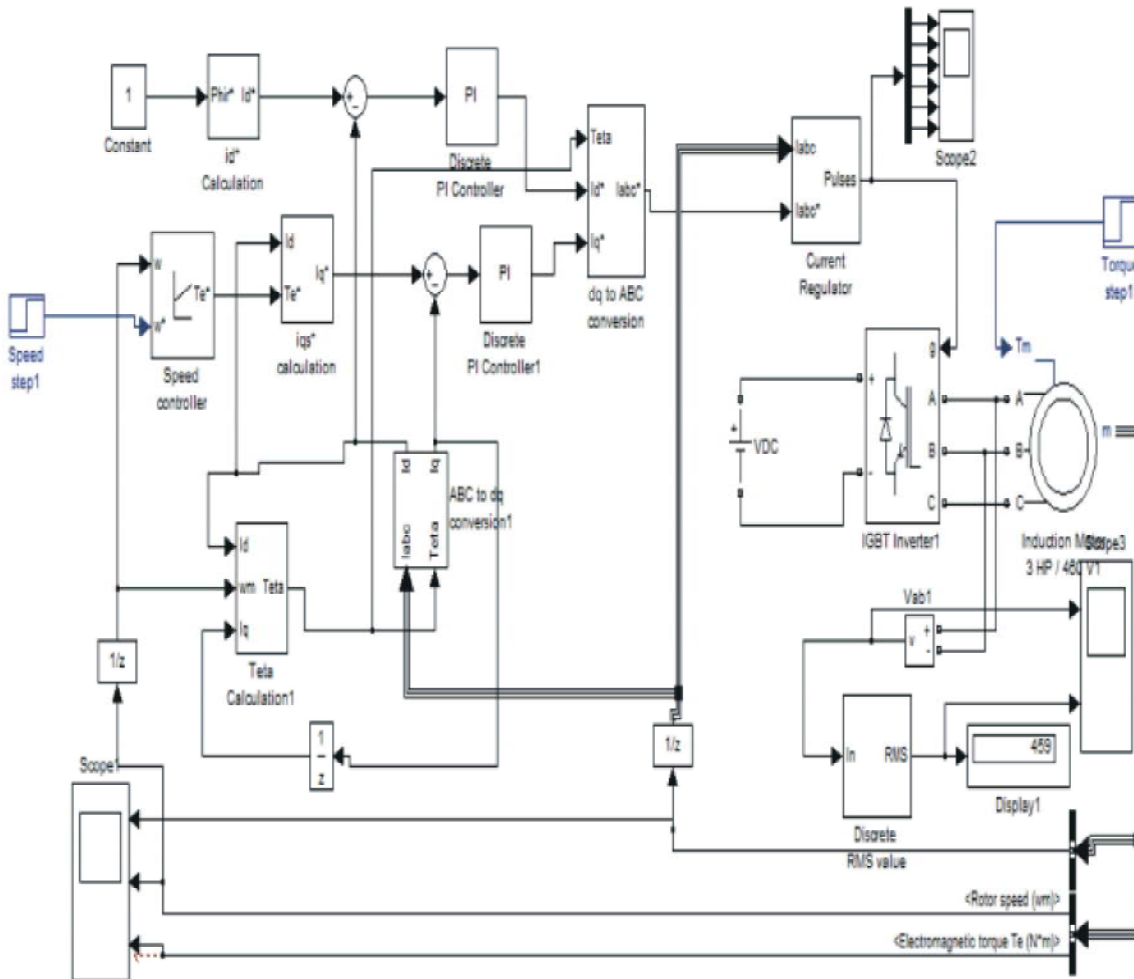


Fig. 9: Matlab/Simulink implementation of Vector Control Induction Motor Drive

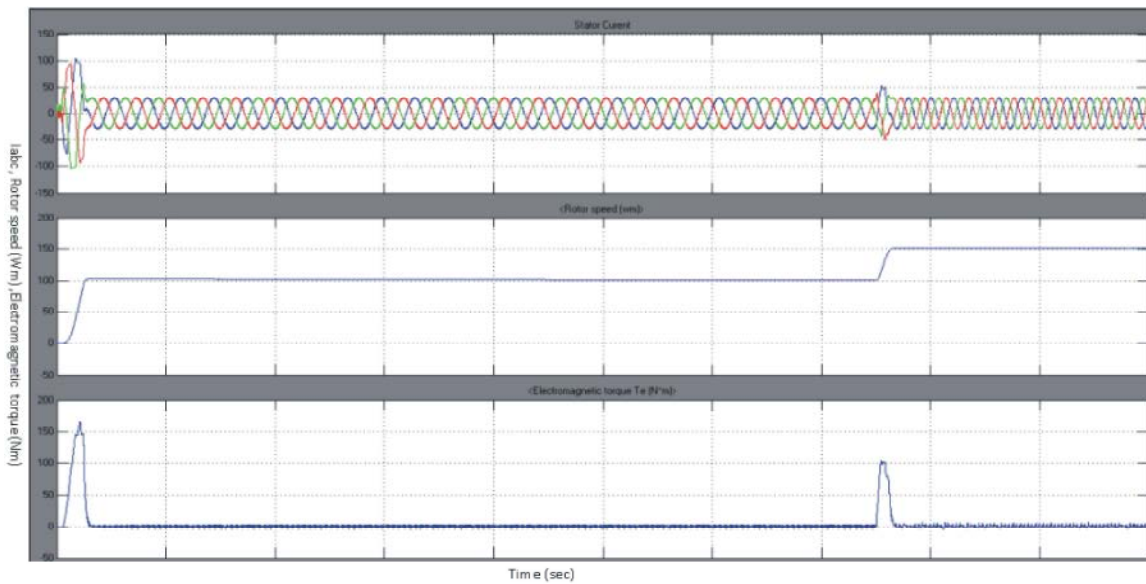


Fig. 10: Stator current, rotor speed and electromagnetic torque waveforms of Vector Control induction motor drive

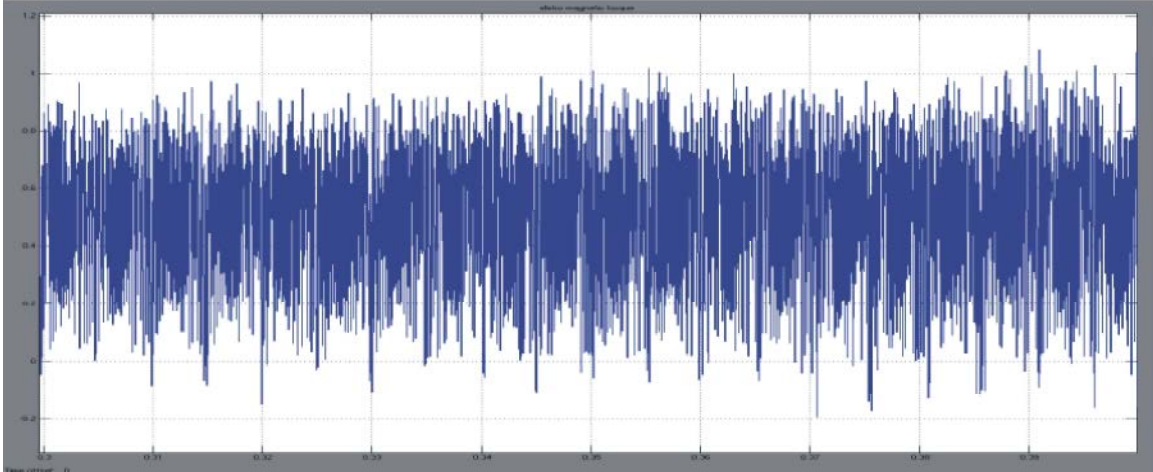


Fig. 11: Ripples in electromagnetic torque

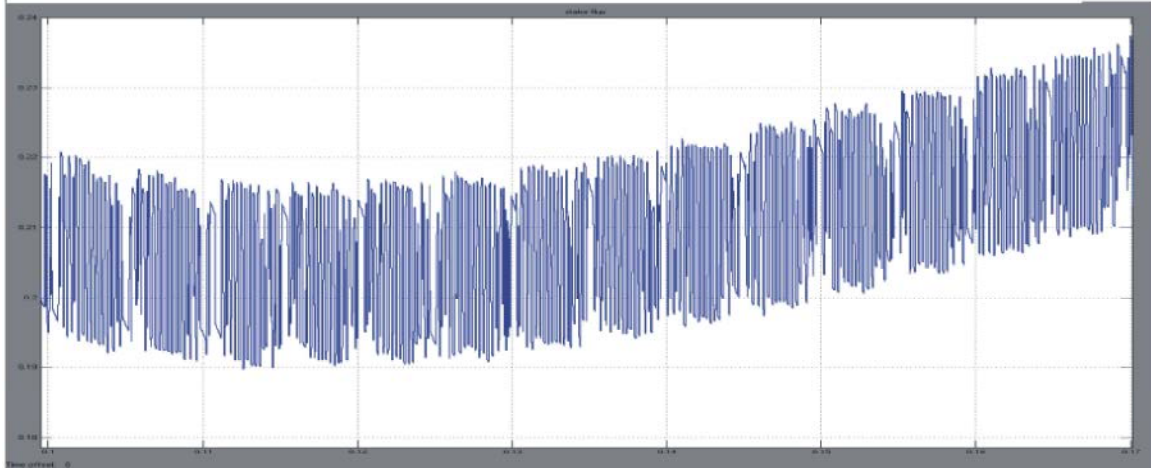


Fig. 12: Ripples in stator flux

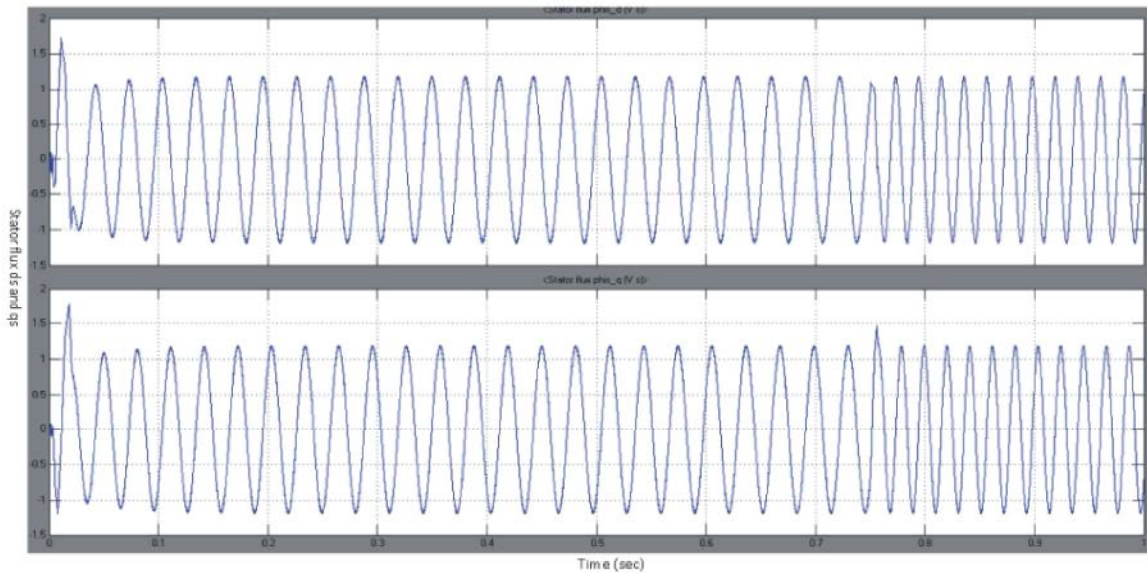


Fig. 13: Stator q-axes and d-axes fluxes which can be controlled independently

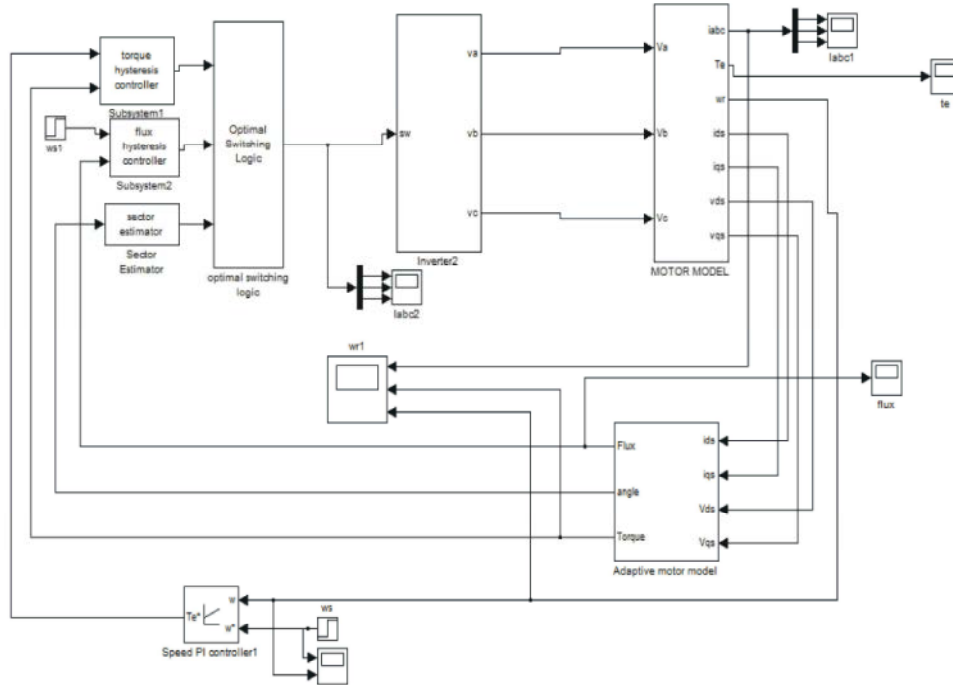


Fig. 14: Matlab/Simulink implementation of Direct Torque Control Induction Motor Drive

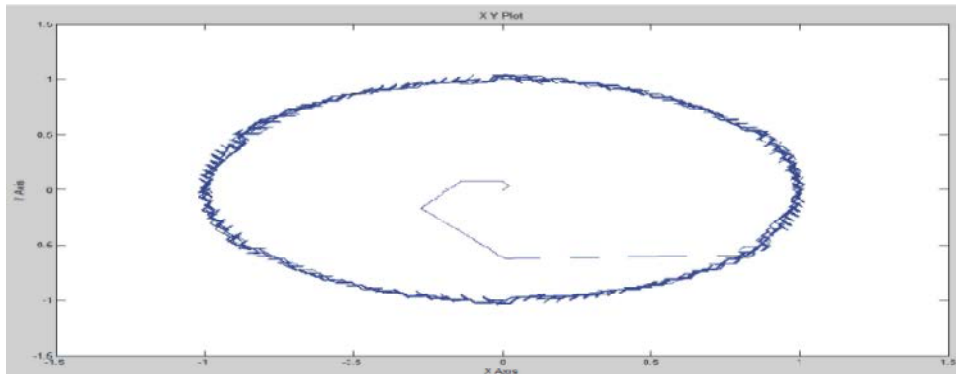


Fig. 15: Stator d-q axes flux in x-y plane

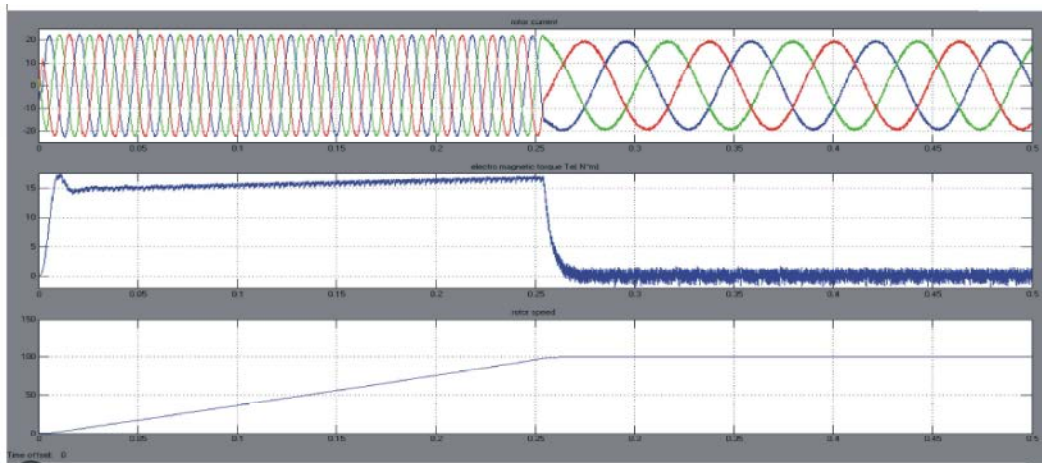


Fig. 16: Simulated waveforms of stator current, electromagnetic torque and rotor speed for DTC induction motor drive

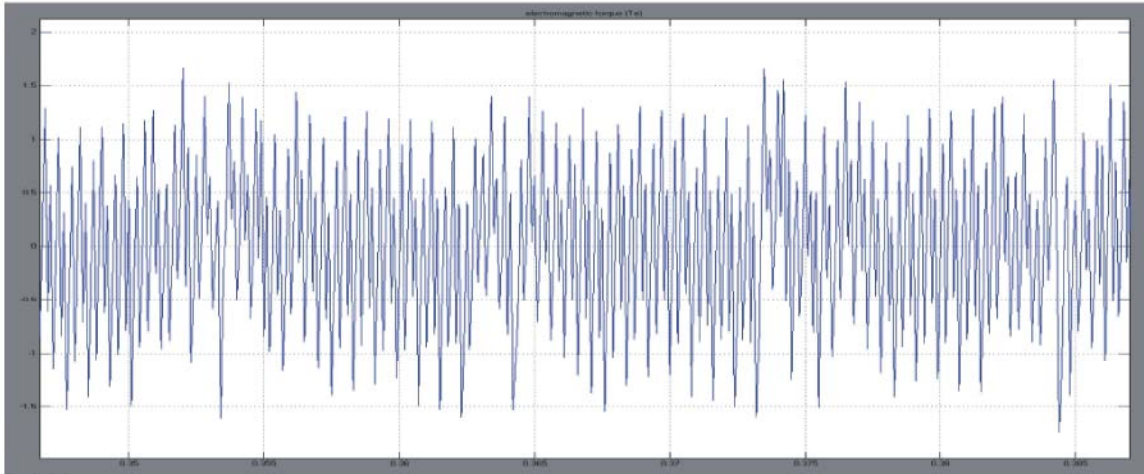


Fig. 4.9: Ripples in electromagnetic torque

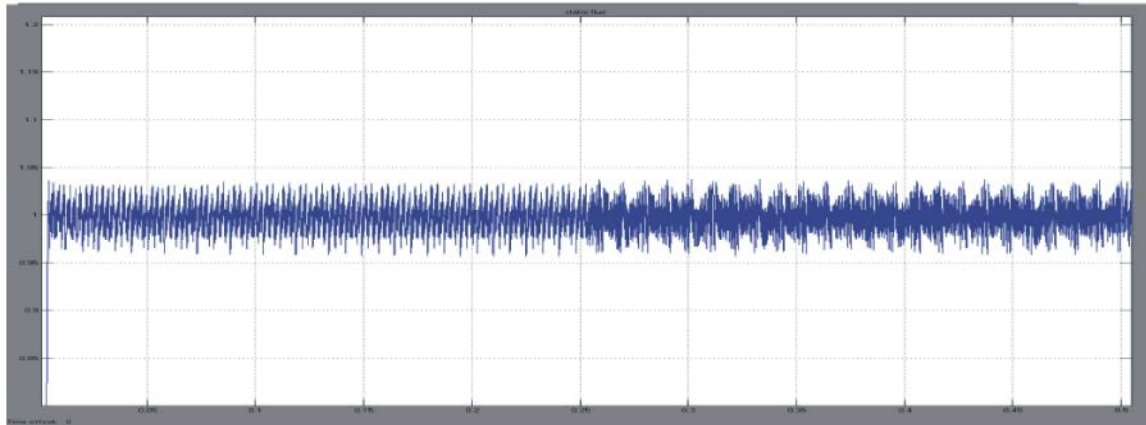


Fig. 18: Ripples in stator flux

CONCLUSION

Induction motor with squirrel cage type is best suited for industrial applications because of their low cost, ruggedness. The advent of the Power Electronics and semiconductor devices has contributed to rapid developments in the field of motor control. The two best methods of the controlling of the induction motor drive are Vector and Direct Torque Controls. This project report briefly explains the Principle of operation of Vector and Direct Torque Controls, their salient feature, advantages and disadvantages. The Vector and Direct Torque Control induction motor drive is implemented using Matlab/Simulink tool box. The simulation results are obtained, analysed and reported. From the simulated results it is observed that the torque ripples in the DTC induction motor drive is high compared to Vector control drive. The transient response is good. with DTC drive.

REFERENCES

1. Bose, Bimal K., Modern Power Electronics and AC Drives, Prentice hall of India.
2. Vas, P., 1998. Sensorless Vector and Direct torque control, Oxford University Press.
3. Takahashi and T. Noguchi, 1986. A new quick response and high efficiency control strategy of an induction motor, IEEE Trans. Ind. Appl., 22(5): 820-827.
4. Marino, P., M. D'Incecco and N. Visciano, 2001. A comparison of direct torque control methodologies for induction motor, Proc. IEEE Porto. Power Tech Conference, Portugal.
5. Takahashi, I. and Y. Ohmori, 1989. High-performance direct torque control of induction motor, IEEE Trans. Ind. Appl., 25(2): 257-264.

6. Habetler, T.G., F. Profumo, M. Pastorelli and L.M. Tolbert, 1992. Direct torque control of induction machines using space vector modulation, *IEEE Trans. Ind. Appl.*, 28(5): 1045-1053.
7. Casadei, D., G. Sera and A. Tani, 0000. Stator flux vector control for high performance induction motor drives using space vector modulation, *Electro motion*, 2(2): 79-86.
8. Lascu, C., I. Boldea and F. Blaabjerg, 2000. A modified direct torque control for induction motor sensorless drive, *IEEE Trans. Industry Applications*, 36(1): 122-130.
9. Casadei, D., G. Sera and A. Tani, 2000. Implementation of a direct torque Control algorithm for induction motors based on discrete space vector Modulation, *IEEE Trans. Power Electronics*, 15(4): 769-777.
10. Shafaq Sherazi and Habib Ahmad, 2014. Volatility of Stock Market and Capital Flow Middle-East *Journal of Scientific Research*, 19(5): 688-692.
11. Kishwar Sultana, Najm ul Hassan Khan and Khadija Shahid, 2013. Efficient Solvent Free Synthesis and X Ray Crystal Structure of Some Cyclic Moieties Containing N-Aryl Imide and Amide, *Middle-East Journal of Scientific Research*, 18(4): 438-443.
12. Pattanayak, Monalisa. and P.L. Nayak, 2013. Green Synthesis of Gold Nanoparticles Using *Elettaria cardamomum* (ELAICHI) Aqueous Extract *World Journal of Nano Science & Technology*, 2(1): 01-05.
13. Chahataray, Rajashree and P.L. Nayak, 2013. Synthesis and Characterization of Conducting Polymers Multi Walled Carbon Nanotube-Chitosan Composites Coupled with Poly (P-Aminophenol) *World Journal of Nano Science and Technology*, 2(1): 18-25.